SUPPLEMENTAL INFORMATION INVENTORY

Figure S1. In vitro analysis of endothelial plexus maturation, related to Figure 1. **(A)** Beads coated with HUVECs before performing the fibrin bead assay. Excess HUVEC cells are seen unattached to beads. **(B-E)** Representative images of the four features of the endothelial plexus that were used for quantitative analysis. (B) Endothelial sprouts originating from a bead as observed after 3 days (arrows). (C) Endothelial tubes (longer and thicker than sprouts) as observed after 5 days. This tube has a branching point at the tip (asterisk). (D) Branchpoints (indicated by asterisks) that result in appearance of new tubes. (E) Anastomosis of two tubes from neighboring beads. **(C' and C")** An additional tube (similar to but different from panel C) photographed in phase contrast and with Hoechst stain (nuclear) fluorescence to more clearly show the organization of multiple endothelial cells surrounding a lumen. **(F-G)** Representative images of HUVEC-coated beads treated with VEGF or VEGF plus CXCL12 in the presence of the CXCR4 inhibitor AMD3100 after 5 days in culture. Treatment with AMD3100 reduced the CXCL12-dependent branching and anastomoses features but not the sprouting induced by VEGF. These images are from the same experiment as Fig. 1E-H. **(H)** Schematic representation of the bead assay. CXCL12 does not induce endothelial sprouting but couples with VEGF-induced sprouting to promote endothelial tube maturation. **(I)** Quantitative PCR analysis of HUVEC gene expression in response to VEGF and CXCL12. VEGF induces the arterial markers *Dll4* and *Efnb2* in a manner that is not influenced by CXCL12, and neither factor alone or together changed expression of the venous markers *CouptfII* (*Nr2f2*) or *EphB4*. n=3 independent samples for each treatment. Data are represented as mean ± SEM. *, $p<0.001$ relative to controls, all other samples are not statistically different from controls.

Figure S2. Expression profiles, related to Figure 2. **(A)** qPCR analysis of *Cxcl12* expression in primary unpassaged embryonic ventricular epicardial cells expanded in culture (Epi) vs. primary embryonic ventricular cardiomyocytes isolated from E13.5 embryos (CM). n=3 independent samples for each. Data are represented as mean ± SEM. *, statistically significant at $p=0.029$. **(B)** *Cxcl12* is expressed in the wall of the aorta. **(C)** Western Blot with an anti-CXCL12 antibody of TCA-precipitated protein from serum-free media conditioned by MEC1 epicardial cells. Recombinant mouse CXCL12 (15, 30 and 60 ng) was included in the blot. **(D)** *Cxcl12* expression in epicardial cells is induced by hypoxia. MEC1 cells (upper panel) or primary epicardial cells (lower panel) were cultured in normoxic (N) or hypoxic (H; 94% N_2, 5% CO_2, 1% O_2) conditions for 6 hr. Gene expression was analyzed by RT-PCR and normalized to b-actin expression. **(E-G)** CXCR4 is expressed in the endocardium (E11.5). **(H-M)** Endothelial cells at E11.5 migrating from the sinus venosus to the myocardium express the venous marker endomucin (EMCN). Panels J-L show higher magnification views of the box area indicated in G-I. **(N)** Whole mount immunohistochemistry for the venous marker EMCN at E12.0. Note that the sprouting EMCN-positive nascent coronary vessels expanding into the ventricle are continuous with the sinus venosus (arrowheads). Abbreviations: endo, endocardium; myo, myocardium, sv, sinus venosus, ra, right atrium, li, liver.

Figure S3. Cardiovascular phenotypes in absence of CXCL12-CXCR4 signaling, related to Figure 3. **(A-B)** Normal distribution of CD31-positive endothelial cells in the dorsal ventricle wall at E12.0. Arrowheads in A' and B' point to nascent endothelial structures. **(C-D)** Dorsal views of control and *Cxcl12* mutant hearts, whole mount CD31 immunostained, at E11.5. The expanded coronary plexus phenotype of *Cxcl12* mutants is the same as *Tie2Cre/Cxcr4* mutants (Fig. 3A,E). **(E)** Quantitation of plexus area on the dorsal and ventral ventricular surfaces, expressed as a percentage. Data are represented as mean ± SEM. n=8 controls and 5 mutants at both time points. *, $p=0.0016$ (E11.5 dorsal) and $p=0.018$ (E12.5 ventral). **(F-M)** Whole mount CD31 immunohistochemistry of hearts isolated at the indicated stages; these are ventral views of the same hearts shown in Fig. 3A-H. At E11.5, because the coronary plexus has not yet reached the ventral heart surface, CD31 staining is only observed in endocardium. Note the expanded

peritruncal and ventral ventricular surface domains at E12.5 and E13.5. **(N-Q)** Sections of control and mutant hearts at E14.5 immunostained with CD31 and neuropilin-1 (NRP1, arterial marker). In the control, intramyocardial vessels are well organized and show expression of the arterial marker; in the mutant, intramyocardial vessels are distorted and show weak NRP1 expression compared to control. **(R-U)** Coronary vasculature defects are not accompanied by compact zone defects. Hematoxylin and eosin stained transverse sections of hearts of the indicated genotypes and ages. Embryos with global deletion of *Cxcl12* or endothelial deletion of *Cxcr4* do not show thinning of the ventricular wall relative to littermate controls. The arrows point to the ventricular septal defect (VSD) in both mutant hearts.

Figure S4. Defects in coronary vessel organization in embryos with disrupted CXCL12 signaling, related to Figure 4. **(A-B)** E17.5 embryos with endothelial-specific deficiency of *Cxcr4* replicate the coronary artery phenotype of *Cxcl12* global mutants. **(C)** *Cxcl12* mutant heart (E15.5) with ink perfusion. The boxed area of this heart is shown in higher magnification in Fig. 3X. **(D-F)** Immunostaining with SM22 showing the presence of normal proximal coronary artery stems in control and two different *Tie2Cre/Cxcr4* mutant hearts. **(G-H)** Freshly dissected hearts at E17.5. The *Cxcl12* mutant heart shows extensive hemorrhage. **(I-L)** Recombination pattern of *Nkx2.5Cre* visualized with the *R26lacZ* reporter. Highly efficient recombination is evident as early as E9.5 in the endocardium and myocardium of the outflow tract (I) and of the atrial and ventricular chambers (J), as also evident at later stages (K,L). The boxed areas of K-L are shown in higher magnification in K', L', and L''. *Nkx2.5Cre* does not recombine in coronary arteries (L') or superficial veins (L'') throughout the mature ventricular wall at E17.5. Abbreviations: ca, coronary artery, cv, coronary vein.

Fig. S1

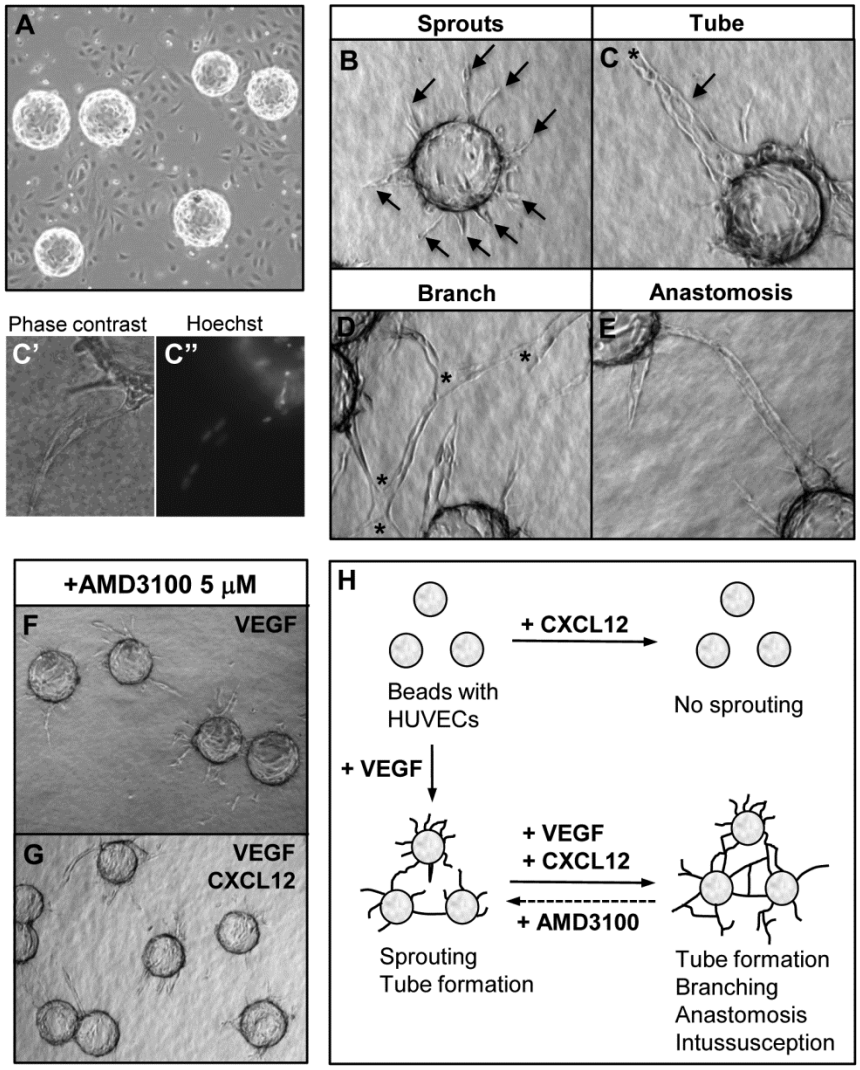
A
Sprouts
Tube
B
C *
Phase contrast
Hoechst
C'
C"
Branch
Anastomosis
D
E
+AMD3100 5 μM
F
VEGF
G
VEGF
CXCL12
H
+ CXCL12
Beads with
HUVECs
No sprouting
+ VEGF
+ VEGF
+ CXCL12
+ AMD3100
Sprouting
Tube formation
Tube formation
Branching
Anastomosis
Intussusception

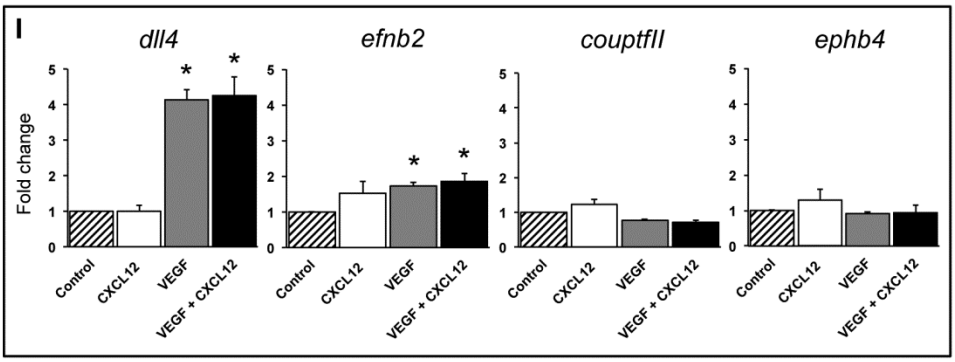
I
dll4
efnb2
couptfII
ephb4
Fold change
Control
CXCL12
VEGF
VEGF + CXCL12

Fig. S2

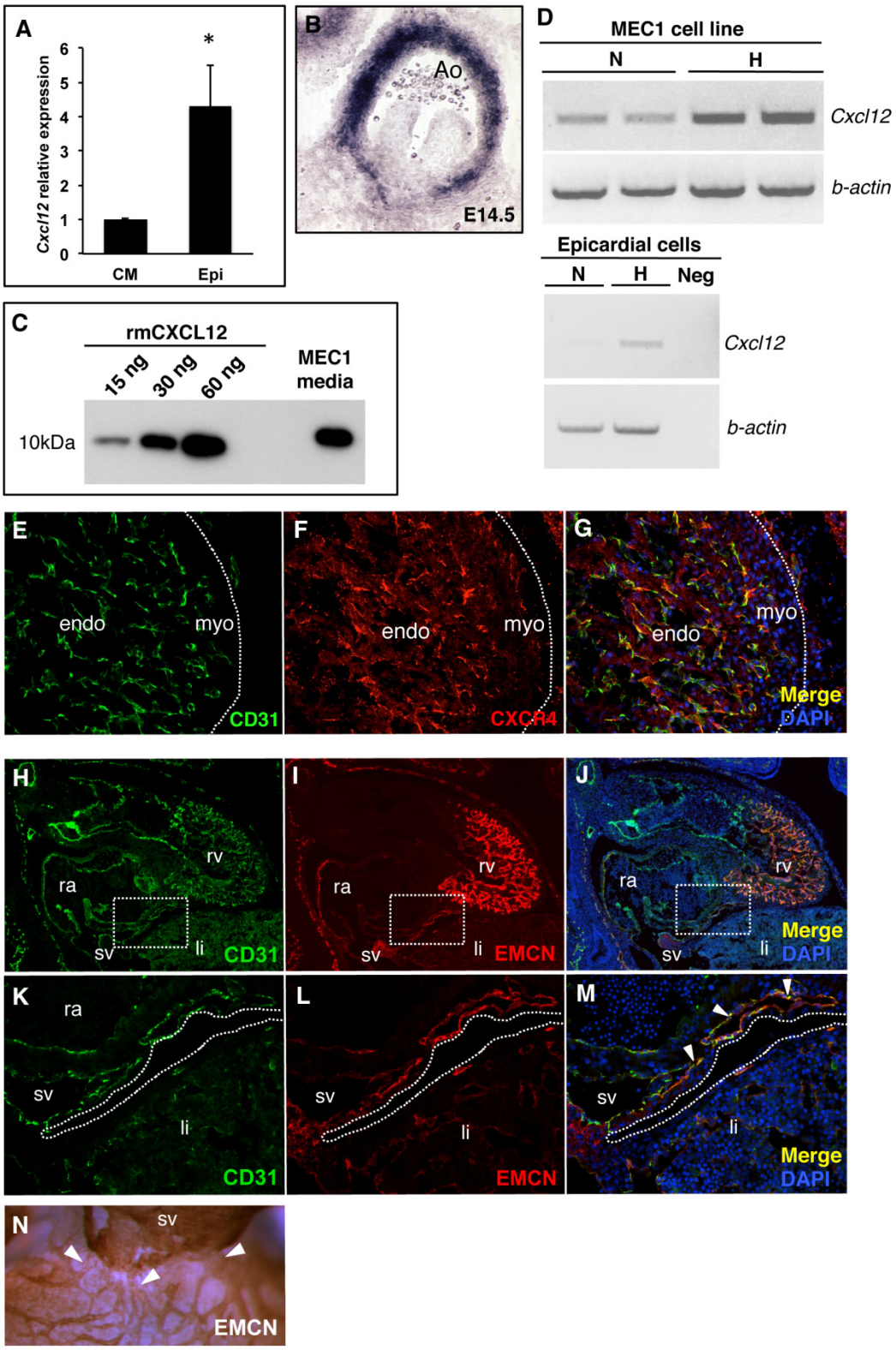
A
Cxcl12 relative expression
6
5
4
3
2
1
0
*
CM
Epi
B
Ao
E14.5
D
MEC1 cell line
N
H
Cxcl12
b-actin
Epicardial cells
N
H
Neg
Cxcl12
b-actin
C
rmCXCL12
15 ng
30 ng
60 ng
MEC1 media
10kDa
E
endo
myo
CD31
F
endo
myo
CXCR4
G
endo
myo
Merge
DAPI
H
rv
ra
sv
li
CD31
I
rv
ra
sv
li
EMCN
J
rv
ra
sv
li
Merge
DAPI
K
ra
sv
li
CD31
L
sv
li
EMCN
M
sv
li
Merge
DAPI
N
sv
EMCN

Fig. S3

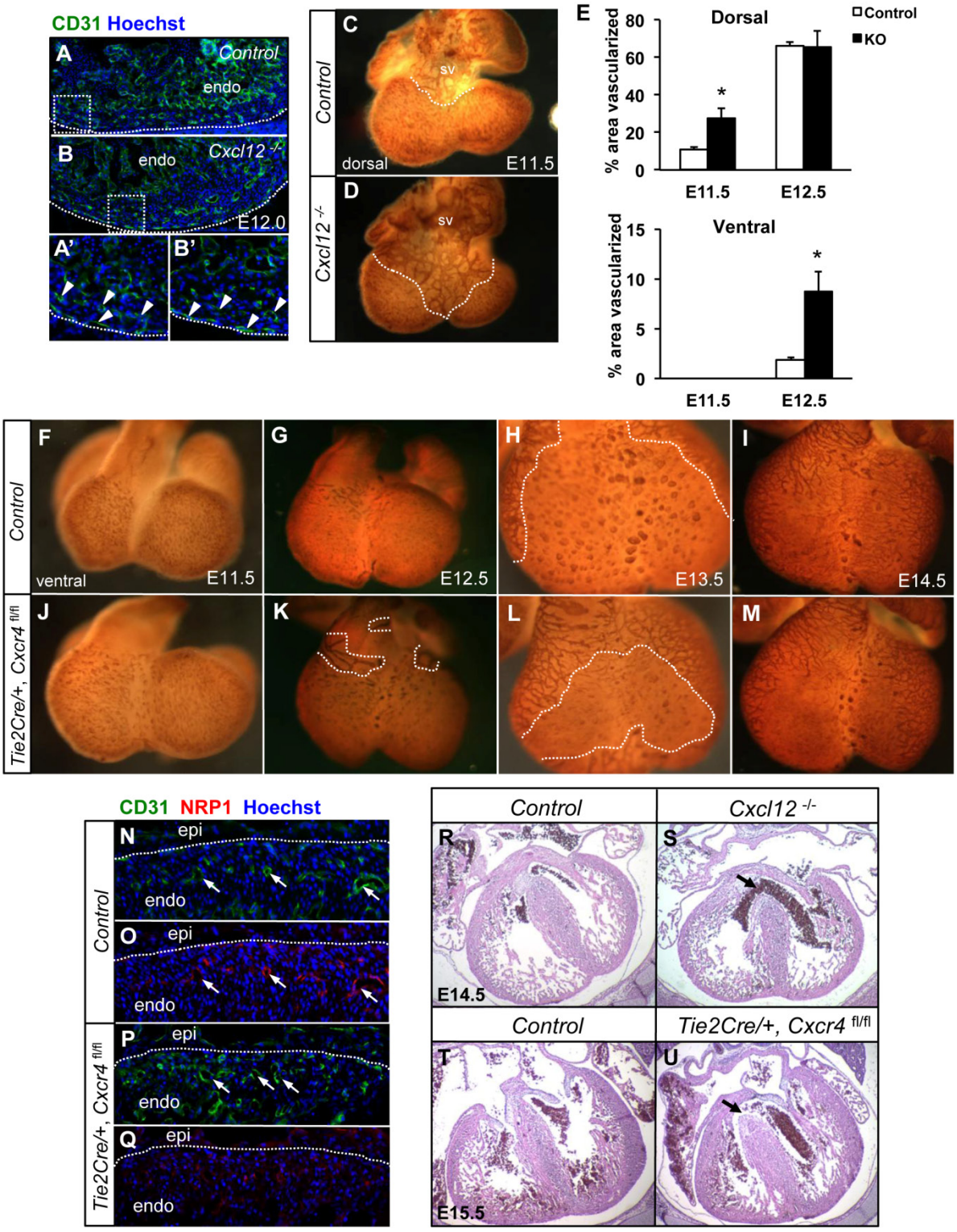
CD31 Hoechst
A
Control
endo
B
endo
Cxcl12 -/-
E12.0
A'
B'
C
Control
sv
dorsal
E11.5
D
Cxcl12 -/-
sv
E
Dorsal
Control
KO
% area vascularized
80
60
40
20
0
*
E11.5
E12.5
Ventral
% area vascularized
15
10
5
0
*
E11.5
E12.5
F
Control
ventral
E11.5
G
E12.5
H
E13.5
I
E14.5
J
Tie2Cre/+, Cxcr4 fl/fl
K
L
M
CD31 NRP1 Hoechst
N
epi
endo
Control
O
epi
endo
P
epi
endo
Tie2Cre/+, Cxcr4 fl/fl
Q
epi
endo
Control
Cxcl12 -/-
R
E14.5
S
Control
Tie2Cre/+, Cxcr4 fl/fl
T
E15.5
U

Fig. S4

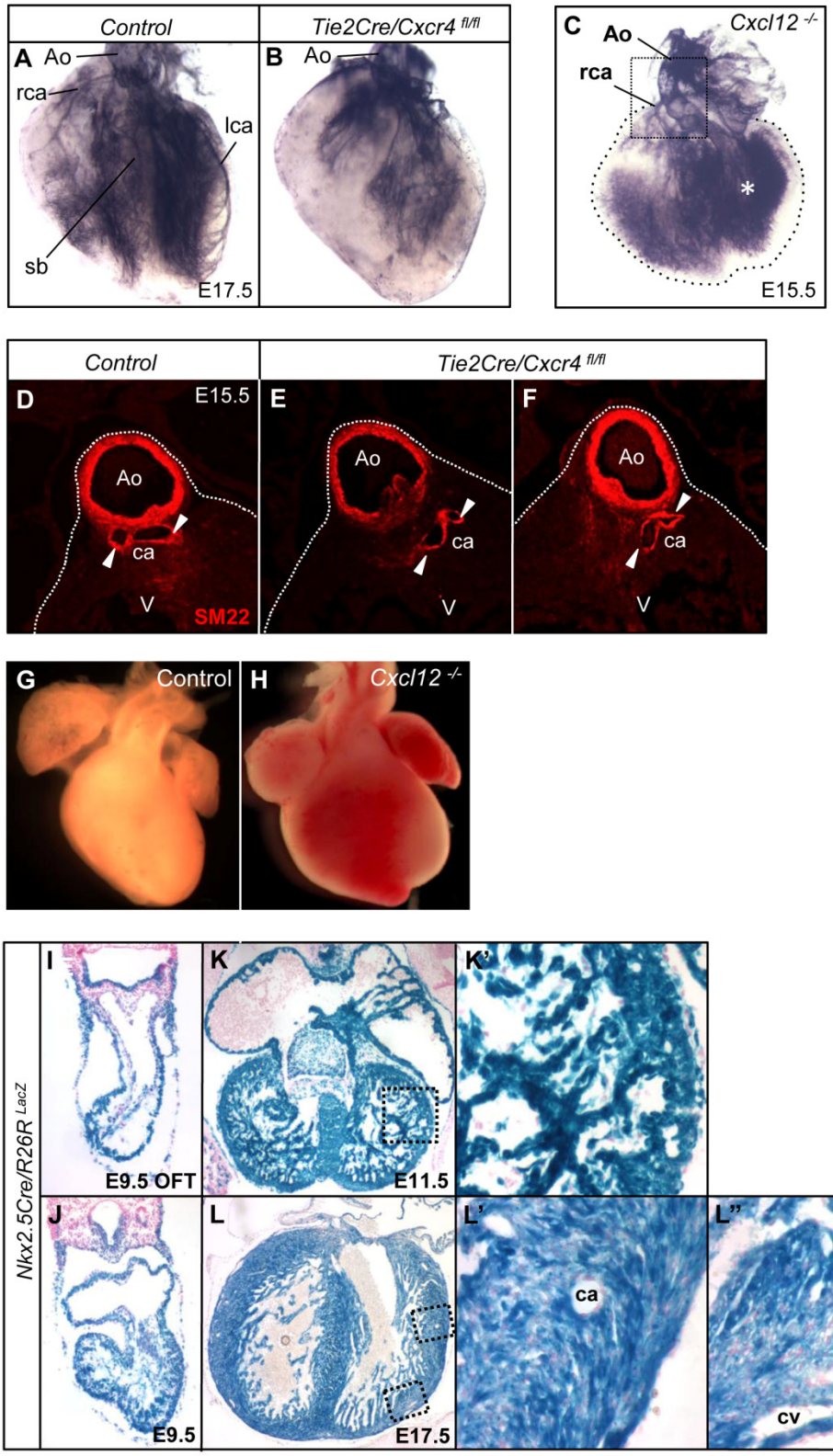
Control
Tie2Cre/Cxcr4 fl/fl
A Ao
rca
lca
sb
E17.5
B Ao
C Ao
Cxcl12 -/-
rca
*
E15.5
Control
Tie2Cre/Cxcr4 fl/fl
D E15.5
Ao
ca
V
SM22
E
Ao
ca
V
F
Ao
ca
V
G Control
H Cxcl12 -/-
Nkx2.5Cre/R26R LacZ
I
E9.5 OFT
K
E11.5
K'
J
E9.5
L
E17.5
L'
ca
L''
cv
cv

Supplemental Experimental Procedures

Epicardial cell culture. The MEC1 mouse embryonic ventricular epicardial cell line was previously described (Li et al., 2011). For isolation of secreted CXCL12, MEC1 cells were cultured until reaching confluence and switched to serum-free DMEM for 24hr. The media was then replaced with fresh serum-free DMEM and collected after 48hr. Total protein was precipitated with trichloroacetic acid and 1mM deoxycholic acid and 30μg of protein was resolved by SDS-PAGE and analyzed by Western analysis. Primary antibody for detection of CXCL12 was from Cell Signaling (1:1000). Recombinant mouse CXCL12 protein (8kDa, R&D Systems) was included as a reference. For *Cxcl12* RNA analysis, MEC1 cells or primary E10.5 embryonic ventricular epicardial cells isolated and grown as described below previously described (Chen et al., 2002) were cultured for 6hr in an incubator culture chamber (CBS Scientific) under normoxic or hypoxic conditions (1% O2/5% CO2/94% N2). Hypoxic media was first sparged with hypoxic gas before use. RNA was isolated and amplified by standard procedures.

Isolation of primary epicardial cells and primary cardiomyocytes for RNA analysis. Primary epicardial cells were grown out from pieces of E13.5 ventricular tissue in DMEM with 10% FBS in gelatin-coated 24-well plates, as previously described (Chen et al., 2002; Li et al., 2011). After 2 days of outgrowth, the culture was switched to serum free overnight. The next day the clumps of ventricular tissue were carefully removed and the remaining epicardial cells were lysed for RNA extraction. Primary ventricular cardiomyocytes were isolated from E13.5 embryonic hearts by pancreatin-collagenase digestion and purified by Percoll gradient centrifugation as described previously (Chen et al., 2002; Kang and Sucov, 2005). The cardiomyocyte fraction was immediately lysed for RNA extraction. cDNA was obtained using MMLV reverse transcriptase (Life Sciences), and *Cxcl12* expression was quantified by qPCR in a Roche Light Cycler 480, normalized to 18S rRNA.

Fibrin bead assay. As previously described (Nakatsu et al., 2003), dextran-coated Cytodex 3 microcarriers (Amersham) were coated overnight with HUVECs (400 cells/bead) in endothelial cell growth media EGM-2 (Lonza). The following day, beads with cells were washed three times with 1ml of endothelial basal media and resuspended at a concentration of 250 coated beads/ml in 2.5 mg/ml fibrinogen (Sigma) with 0.15 units/ml of aprotinin (Sigma). The fibrinogen/bead solution was added to the wells of a 24-well plate containing thrombin (Sigma) and allowed to clot for 5 min at room temperature and then at 37°C and 5% CO_2 for 20 min. 1ml of endothelial basal media containing 2% FBS with or without VEGF (R&D Systems; 20ng/ml), CXCL12 (R&D Systems; 100ng/ml), or AMD3100 (Sigma, 5μM) was added to each well. Normal adult human primary dermal fibroblasts (ATCC PSC-201-012; 20,000 cells/well) were plated on top of the clot. Media was changed every other day. Bead assays were monitored for up to 7 days. Beads were photographed at 5 x magnification under phase contrast. Sprout number, tube number, branching points and anastomoses (as exemplified in Fig. S1) were manually quantified from at least 10 microscopic fields per well in which each field contained 4-10 beads. Tubes and anastomosis formed between tubes were not counted if beads were closer than one bead diameter. Experiments were repeated 3 separate times.

HUVEC RNA analysis. HUVECs (P3 to P5) were grown in EGM-2 (Lonza) and plated in 12-well plates (10,000 cells/cm^2). At 75% confluence cells were switched to basal media with 2% FBS overnight. The next day they were treated overnight with VEGF (20ng/ml), CXCL12 (100 ng/ml), or a combination of both. Total RNA was extracted (Zymo Research), converted to cDNA, and analyzed by qPCR (Roche) normalized to 18s rRNA expression.

In situ hybridization. Embryos were fixed overnight in 4% PFA, washed in PBS, cryoprotected overnight in sucrose 10% followed by sucrose 30%/OCT 20%, and embedded in OCT. Tissue sections (8μ) were fixed in 4% paraformaldehyde for 10 min on ice, rinsed in PBS, and acetylated in 0.1M triethanolamine/0.25% acetic anhydride for 15 min at room temperature. Sections were prehybridized with hybridization buffer (Enzo Life Sciences) for 30-60min at 58°C in a chamber hydrated with 5 X SSC/50% formamide. Digoxigenin (DIG)-labeled (Roche) antisense probes or sense controls were diluted to 250ng/ml in hybridization buffer, denatured at 85°C for 5 min, cooled and added to slides, which were incubated overnight at 58°C in a hybridization oven. After hybridization, slides were washed with 2X SSC for 30 min at room temperature. Non-hybridized probes were digested with RNaseA (Roche) in 2X SSC at 37°C for 30min, followed by 0.1X SSC for 1h at 65°C. Sections were then blocked with TBS/0.1% Tween/ 5% sheep serum (Sigma) and incubated overnight with alkaline phosphatase-conjugated anti-DIG primary antibody (Roche) diluted in blocking solution. Signal was detected by NBT-BCIP (Roche) diluted in TE buffer containing $MgCl_2$ 50mM and levamisole 0.5 mg/ml.

Mice. All mice were housed and bred within the animal facility at the University of Southern California in accordance with Institutional Animal Care and Use Committee guidance. ICR and C57BL/6 mice (Harlan) were used for wild-type expression analysis. All mouse lines used in this study have been described previously: *Cxcl12* mutant (Ara et al., 2003), conditional *Cxcr4* (Nie et al., 2004), *Tie2Cre* transgenic (Kisanuki et al., 2001), *Nfatc1Cre* (Zhou et al., 2002), *Nkx2.5Cre* knock-in (Moses et al., 2001), and conditional *R26lacZ* and *R26YFP* (Soriano, 1999). The *Cxcl12* line was maintained on a C57BL/6 background; all other lines were on mixed and unspecified strain backgrounds. Noon of the day when vaginal plug was observed was considered as E0.5.

India ink coronary artery perfusion. Embryos were collected over the E15.5- E17.5 period in PBS containing 2μg/ml heparin. Immediately, the thoracic cavities were cut and transferred to DMEM/10%FBS/heparin on ice. Hearts were carefully dissected from the surrounding tissues and then placed on an inverted Petri dish and gently dried to avoid movement during perfusion. India ink was diluted in PSB/heparin and injected from the ascending aorta with a borosilicate glass tube thinned to the appropriate diameter attached to a mouth pipette. India ink was slowly injected by minute puffs of breath during diastolic intervals. Hearts were fixed in 4% PFA, dehydrated, cleared in BABB (benzyl alcohol: benzyl benzoate, 1:1) and imaged with a stereomicroscope.

Whole mount immunohistochemistry. Hearts were fixed overnight in 4% PFA, permeabilized in PBS with 0.5% NP-40, dehydrated in a methanol series, incubated in methanol/hydrogen peroxide, rehydrated and blocked in PBSST (PBS containing 5% BSA and 0.1% Triton X-100). The primary antibody was rat anti-mouse PECAM (BD, 1:100) or endomucin (Abcam, 1:100). Biotinylated goat anti-rat IgG (Santa Cruz, 1:500) was used followed by streptavidin-peroxidase complex (Vectastain ABC kit, Vector). Antibody and ABC reagent incubations were carried out in PBSST at 4°C overnight. Following overnight incubations, hearts were washed five times (1 hour each at 4°C) with PBSST. Immunoreactivity was visualized with DAB substrate (Invitrogen). Image J was used to determine the percentage of the dorsal and ventral surfaces covered by coronary elements, standardized to embryo crown-rump length.

Immunofluorescence. Embryos were fixed in PFA 4% and cryoprotected overnight in sucrose 10% followed by sucrose 30%/OCT 20%, and embedded in OCT. Cryosections (8-10μ) were permeabilized in PBS containing 0.1% Triton X-100 and blocked with casein solution (Vector). Primary antibodies, diluted in PBS containing 1% BSA and 10% serum, were anti mouse CD31

(BD, 1:100), endomucin (Santa Cruz, 1:100), neuropilin-1 (Santa Cruz, 1:50), and SM22 (Abcam, 1:100). Appropriate negative controls were performed in the absence of the primary antibody. Signal was detected with Alexa Fluor-546 and -488 conjugated secondary antibodies (Molecular Probes, 1:250).

Supplemental References

Ara, T., Nakamura, Y., Egawa, T., Sugiyama, T., Abe, K., Kishimoto, T., Matsui, Y., and Nagasawa, T. (2003). Impaired colonization of the gonads by primordial germ cells in mice lacking a chemokine, stromal cell-derived factor-1 (SDF-1). Proc Natl Acad Sci U S A *100*, 5319-5323.

Chen, T., Chang, T.C., Kang, J.O., Choudhary, B., Makita, T., Tran, C.M., Burch, J.B., Eid, H., and Sucov, H.M. (2002). Epicardial induction of fetal cardiomyocyte proliferation via a retinoic acid-inducible trophic factor. Dev Biol *250*, 198-207.

Kang, J.O., and Sucov, H.M. (2005). Convergent proliferative response and divergent morphogenic pathways induced by epicardial and endocardial signaling in fetal heart development. Mech Dev *122*, 57-65.

Kisanuki, Y.Y., Hammer, R.E., Miyazaki, J., Williams, S.C., Richardson, J.A., and Yanagisawa, M. (2001). Tie2-Cre transgenic mice: a new model for endothelial cell-lineage analysis in vivo. Dev Biol *230*, 230-242.

Li, P., Cavallero, S., Gu, Y., Chen, T.H.P., Hughes, J., Hassan, A.B., Bruning, J., Pashmforoush, M., and Sucov, H.M. (2011). IGF signaling directs ventricular cardiomyocyte proliferation during embryonic heart development. Development *138*, 1795-1805.

Moses, K.A., DeMayo, F., Braun, R.M., Reecy, J.L., and Schwartz, R.J. (2001). Embryonic expression of an Nkx2-5/Cre gene using ROSA26 reporter mice. Genesis *31*, 176-180.

Nakatsu, M.N., Sainson, R.C., Aoto, J.N., Taylor, K.L., Aitkenhead, M., Perez-del-Pulgar, S., Carpenter, P.M., and Hughes, C.C. (2003). Angiogenic sprouting and capillary lumen formation modeled by human umbilical vein endothelial cells (HUVEC) in fibrin gels: the role of fibroblasts and Angiopoietin-1. Microvasc Res *66*, 102-112.

Nie, Y., Waite, J., Brewer, F., Sunshine, M.J., Littman, D.R., and Zou, Y.R. (2004). The role of CXCR4 in maintaining peripheral B cell compartments and humoral immunity. J Exp Med *200*, 1145-1156.

Soriano, P. (1999). Generalized lacZ expression with the ROSA26 Cre reporter strain. Nat Genet *21*, 70-71.

Zhou, B., Cron, R.Q., Wu, B., Genin, A., Wang, Z., Liu, S., Robson, P., and Baldwin, H.S. (2002). Regulation of the murine Nfatc1 gene by NFATc2. J Biol Chem *277*, 10704-10711.